Keratin Isotypes Control Desmosome Stability and Dynamics through PKCα

Fanny Loschke[1], Melanie Homberg[1] and Thomas M. Magin[1]

Expression and interaction of desmosomal components and keratins provide stable cell cohesion and protect the epidermis against various types of stress. The differentiation-specific isotype composition of the keratin cytoskeleton and desmosomes is regarded as a major determinant of adhesive strength. In support, wound healing is characterized by a transient decrease in desmosomal adhesion accompanied by increased expression of keratins K6/K16/K17 at the expense of K1/K10. The significance of altered keratin expression for desmosomal composition and adhesion remains incompletely understood at a mechanistic and functional level. Here, we investigated the respective contribution of K5/K14 or K6/K17 to desmosome adhesion, on their stable re-expression in keratinocytes lacking all keratins. This revealed that K5/K14 filaments support stable desmosomes, whereas "wound healing" keratins K6/K17 induce elevated protein kinase C alpha–mediated desmosome disassembly and subsequent destabilization of epithelial sheets. Moreover, our data suggest that K5/K14 sequester protein kinase C alpha in the cytoplasm, whereas K6/K17 or the absence of all keratins enables protein kinase C alpha translocation to the plasma membrane and induction of desmosome disassembly. Gain- and loss-of-function experiments support a major role of K5 in desmosome stability control via protein kinase C alpha. Our data show that keratin isotypes differently and specifically regulate wound healing and invasion by modulating intercellular adhesion.

Journal of Investigative Dermatology (2016) **136,** 202-213; doi:10.1038/JID.2015.403

INTRODUCTION

The epidermis has evolved to protect the body against mechanical stress, infections, and dehydration by virtue of strong intercellular adhesion among keratinocytes. Stable intercellular adhesion and force resilience are controlled by several types of cell adhesion complexes attached to the cytoskeleton. Among these, the keratin-desmosome scaffold has a dual role in regulating epidermal differentiation through crosstalk with growth factors, in addition to mediating intercellular adhesion (Homberg and Magin, 2014; Loschke et al., 2015; Simpson et al., 2011). To adapt keratinocyte adhesion and function to requirements of differentiation, wound healing, and pathogenesis, the keratin-desmosome complex requires remodeling at the level of protein composition, interactions, and posttranslational modifications (PTMs) (Albrecht et al., 2015; Simpson et al., 2011). Keratins (K) are encoded by a large gene family of 28 type I and 26 type II keratins expressed in a pairwise fashion to ensure the formation of the intermediate filament cytoskeleton in all epithelia from heterodimeric subunits in a cell-specific and differentiation-dependent manner (Hesse et al., 2004; Magin et al., 2007). Ultimately, keratin intermediate filaments are organized as networks that attach to desmosomes and hemidesmosomes, thereby contributing to the mechanical and signaling properties of epithelia (Pan et al., 2013; Windoffer et al., 2011). The basal, proliferative compartment of the epidermis predominantly expresses the keratin pair K5/K14, which on terminal differentiation is replaced by K1/K10. This default pattern is altered during barrier disruption, wounding, tissue regeneration, and malignant transformation, conditions that require transient decreased intercellular adhesion, enhanced proliferation, and migration of keratinocytes. In these settings, K6, K16, and K17 are rapidly and transiently expressed at the expense of K1/K10. Although in vitro data show that K5/K14 protein complexes are much more stable than those between K6/K16/K17 (Hatzfeld and Franke, 1985), the contribution of keratin isotypes to desmosome-mediated keratinocyte adhesion during differentiation and wound healing is not fully resolved. During epidermal injury, re-epithelialization is the most crucial process, as its failure underlies chronic, nonhealing wounds, a clinically highly relevant problem (Gurtner et al., 2008). Re-epithelialization involves altered adhesion, migration, and proliferation of keratinocytes at the wound edge to enable wound closure and restoration of the epidermal barrier (Shaw and Martin, 2009). Among the earliest changes detectable in keratinocytes at the wound margin are diminished contacts of keratins to desmosomal proteins and loss of desmosome hyperadhesion (Garrod et al., 2005; Paladini et al., 1996), followed by increased keratinocyte migration mediated by a K6-Src sequestration mechanism (Rotty and Coulombe, 2012). Delayed wound healing in protein kinase C alpha ($PKC\alpha^{-/-}$) mice supports a major contribution of PKCα in

[1]*Institute of Biology and Translational Center for Regenerative Medicine, University of Leipzig, Leipzig, Germany*

Correspondence: Thomas M. Magin, Translational Center for Regenerative Medicine (TRM) and Institute of Biology, Division of Cell and Developmental Biology, University of Leipzig, Talstrasse 33, D-04103 Leipzig, Germany. E-mail: thomas.magin@uni-leipzig.de

Abbreviations: DP, desmoplakin; Dsg, desmoglein; K, keratin; KIF, keratin intermediate filament; KtyI, keratin type I gene cluster; KtyII, keratin type II gene cluster; PKCα, protein kinase C alpha; PKP, plakophilin; PM, plasma membrane; WB, Western blotting; WT, wild-type

Received 20 March 2015; revised 4 September 2015; accepted 11 September 2015; accepted manuscript published online 12 October 2015

regulating desmosome adhesion. Conversely, overexpression of PKCα accelerated wound healing by decreasing desmosome adhesion (Thomason et al., 2012). Yet, these studies have not examined expression and contribution of keratin isotypes to PKCα regulation.

Altogether, these findings raise the question to which extent the composition and abundance of keratin intermediate filaments contribute to desmosome adhesion and epithelial stability. Previously, we reported that the absence of all keratins in keratinocytes rendered epithelial sheets fragile on exposure to mechanical stress, but that moderate expression levels of K5/K14 rescued sheet integrity (Kroger et al., 2013). Also, our data indicated that keratins sequester PKCα through the scaffold protein Rack1, thereby limiting phosphorylation of desmosomal proteins necessary for desmosome stability (Kroger et al., 2013). To further dissect isotype-specific keratin functions, we established stable keratinocyte cell lines re-expressing type I keratins K14 or K17 or type II keratins K5 or K6 in the corresponding keratin null background. This revealed that cells expressing K6 or K17 show elevated, PKCα-mediated desmosome disassembly and subsequent destabilization of epithelial sheets. In contrast, keratinocytes expressing K5 or K14 displayed stable desmosomes, suggesting that expression of "wound healing" keratins weakens intercellular adhesion. Furthermore, gain- and loss-of-function studies suggest that the type II keratin K5 is a major determinant of desmosome stability, whereas type I keratins seem to play a minor role.

RESULTS AND DISCUSSION

Expression of K14, but not of K17, stabilizes desmosomes

Recently, lack of keratins in the epidermis of mice was found to diminish the size and number of desmosomes along the plasma membrane (PM), accompanied by accumulation of desmosomal proteins in the cytoplasm (Bar et al., 2014; Kroger et al., 2013). Mechanistic studies using cultured keratinocytes showed that under steady-state conditions, keratins restrict desmosomal protein phosphorylation in a PKCα-dependent manner and thereby stabilize desmosomes at the PM (Kroger et al., 2013). To further examine the contribution of different keratin isoforms to epithelial integrity, maintenance, and dynamics of junctions, we established different cell lines expressing only distinct keratin isotypes. By lentiviral transduction of cells lacking the entire keratin type I gene cluster (KtyI$^{-/-}$), we generated cells expressing either K14 (KtyI$^{-/-}$K14; K14 cells) or K17 (KtyI$^{-/-}$K17; K17 cells) as the sole type I keratin. In the background of cells lacking the entire keratin type II gene cluster (KtyII$^{-/-}$), we expressed K5 (KtyII$^{-/-}$K5; K5 cells) or K6 (KtyII$^{-/-}$K6; K6 cells) as the sole type II keratin.

Genetically, KtyI$^{-/-}$ cells lack all type I keratin genes but maintain type II keratin gene expression (Ramms et al., 2013). At the mRNA level, no type I keratin is detectable, as shown for K14 and K17, whereas type II keratin genes were transcribed, as shown for K5 and K6 (Supplementary Figure S1a online). Western blotting (WB) revealed the absence of type I and the strong reduction of type II keratins at the protein level (Figure 1a). Immunostainings confirmed the absence of keratin filaments in KtyI$^{-/-}$ compared with wild-type (WT) cells (Figure 1b–c‴). In KtyI$^{-/-}$ cells, after stable transduction with K14 or K17 cDNAs, also K5 and K6 are present at the protein level, next to K14 or K17 (Figure 1a–a′). WB of total protein lysates showed similar levels of K14 (38%) and K17 (31%), relative to their expression in WT cells (Figure 1a′). The level of K5 protein is higher in K14 compared with K17 cells, the amount of K6 is higher in K17 compared with K14 cells (Figure 1a′). At the same time, the overall amount of unsoluble keratin proteins was slightly diminished in K17 cells compared with K14 cells, as documented by Coomassie Blue staining of the IF-enriched protein fractions separated by SDS-PAGE (Supplementary Figure S1b–b′). The unaltered mRNA levels of these type II keratins in both K14 and K17 cells point toward a posttranslational regulatory mechanism (Supplementary Figure S1a). Analysis of protein half-life times, after cell treatment with cycloheximide and subsequent WB, revealed increased stability of K5 and accelerated degradation of K6 in the presence of K14 and increased stability of K6 along with increased degradation of K5 in the presence of K17 (Supplementary Figure S1c–c′). In support, the stability of heteromeric complexes between distinct keratins is different in vitro, although all type I keratins can pair with all type II keratins (Hatzfeld and Franke, 1985). Our data indicate that specific keratin pairs, such as K5/K14 and K6/K17, are formed preferentially in vivo. Furthermore, quantitative PCR and WB suggest that selectivity of certain keratin pairs occurs at the protein level and is not due to differences at the transcript level (Figure 1a–a′, Supplementary Figure S1a–c′). Whether this difference in stability is related to differences in affinities or is affected by different PTMs of keratins remains to be shown. Irrespective of composition, confocal microscopy of K5, K14, K6, and K17 showed WT-like cytoskeletal organization in both cell lines (Figure 1d–e‴).

To investigate whether intercellular adhesive strength depends on distinct keratin isotypes, a mechanical cell dissociation assay was performed. In this assay, confluent cell monolayers were lifted from the cell culture dish by dispase treatment and subjected to mechanical stress (Calautti et al., 1998). Loss of all keratins weakens intercellular adhesive strength to a significant extent, as shown by a greater than 100-fold increase in the number of sheet fragments, compared with WT controls (Homberg et al., 2015; Kroger et al., 2013) (Figure 2a, a′, a‴). Presently, we cannot exclude a partial contribution from cytolyzing, in addition to disturbed desmosomes, to the impaired epithelial sheet integrity in the mechanical dispase assay. The expression of K14 restored epithelial sheet integrity to a significant extent, in contrast to K17 cells (Figure 2a″–a‴). Confocal microscopy revealed a considerable decrease of DP1/2 at the PM and accumulation of DP1/2 in the cytoplasm of KtyI$^{-/-}$ and K17 cells, compared with WT and K14 cells (Figure 2b–b‴). Desmoglein (Dsg) and desmoplakin (DP) colocalize to some extent in the cytoplasm of K17 cells (Supplementary Figure S2a online), indicating that some desmosomal proteins are internalized together (McHarg et al., 2014). Similar to KtyI$^{-/-}$ and KtyII$^{-/-}$ cells (Homberg et al., 2015; Kroger et al., 2013) (Supplementary Figure S2c), the level of desmosomal proteins in K17 cells is strongly decreased, ranging from 76% for Dsg1/2, 40% for plakophilin 1, 45% for plakophilin 3, to 88% for DP1/2 after 72 hours, compared

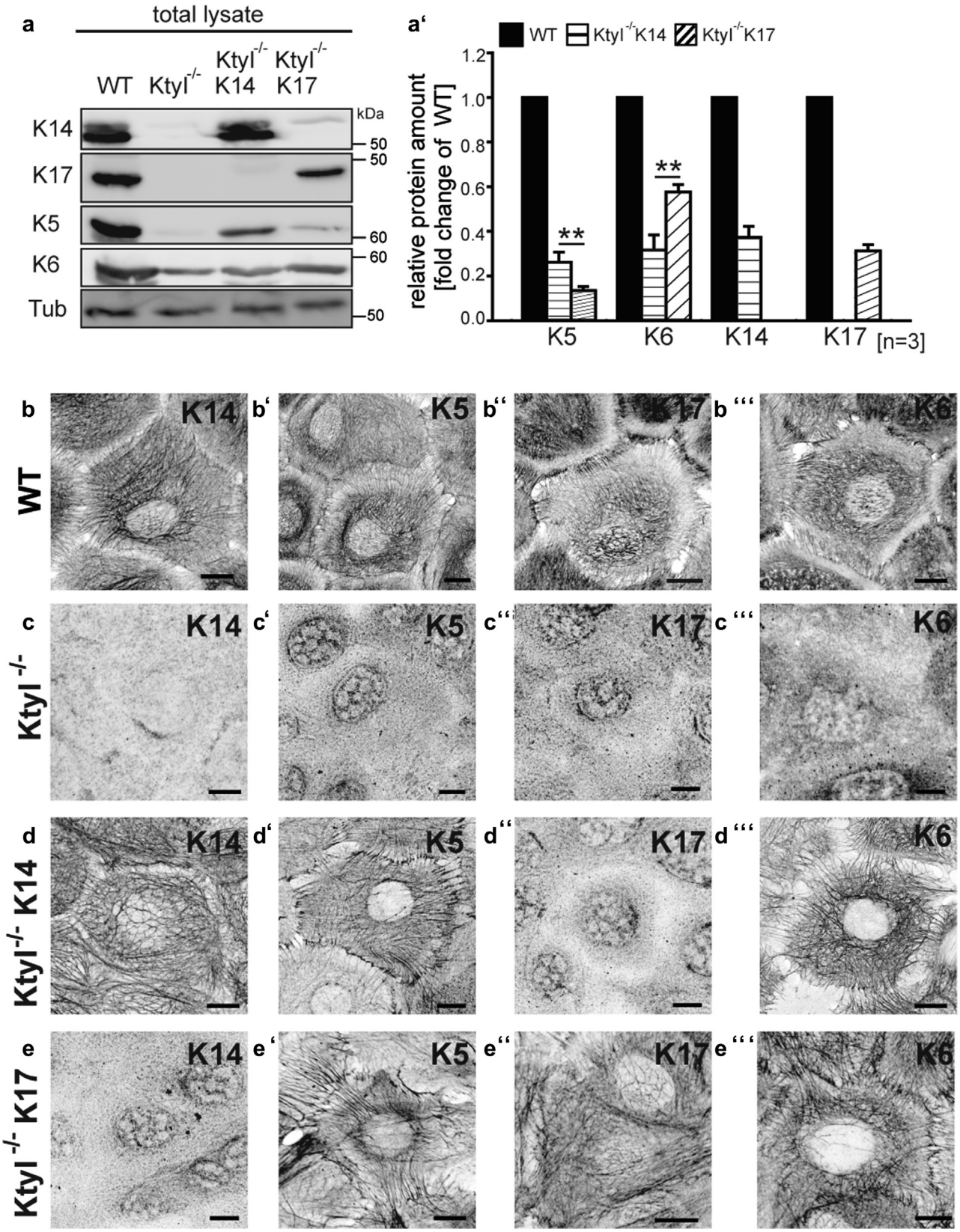

Figure 1. Keratin expression in WT, KtyI$^{-/-}$, K14 and K17 cells. (**a**–**a**′) WB of keratin proteins confirmed re-expression of K14, K5, and K6 in K14 cells and K17, K5, and K6 in K17 cells. Keratin amounts in rescue cells were determined by densitometric analysis of keratin bands relative to the loading control tubulin and calculated as fold-change to the amount of K5, K6, K14, or K17 expressed in WT controls. Note similar levels of K14 and K17, relative to their expression in WT cells, but disparate levels of K5 and K6 (**a**′). (**b**–**e**‴) Immunostaining of keratins showed the absence of filaments in KtyI$^{-/-}$ cells (**c**–**c**‴). K14 cells display KIF positive for K14, K5, and K6 (**d**–**d**‴) and K17 cells display KIF positive for K17, K5, and K6 (**e**–**e**‴) in a WT-like manner (compared with b–b‴). KIF, keratin intermediate filaments; WB, Western blotting; WT, wild-type. Scale bars: 10 μm.

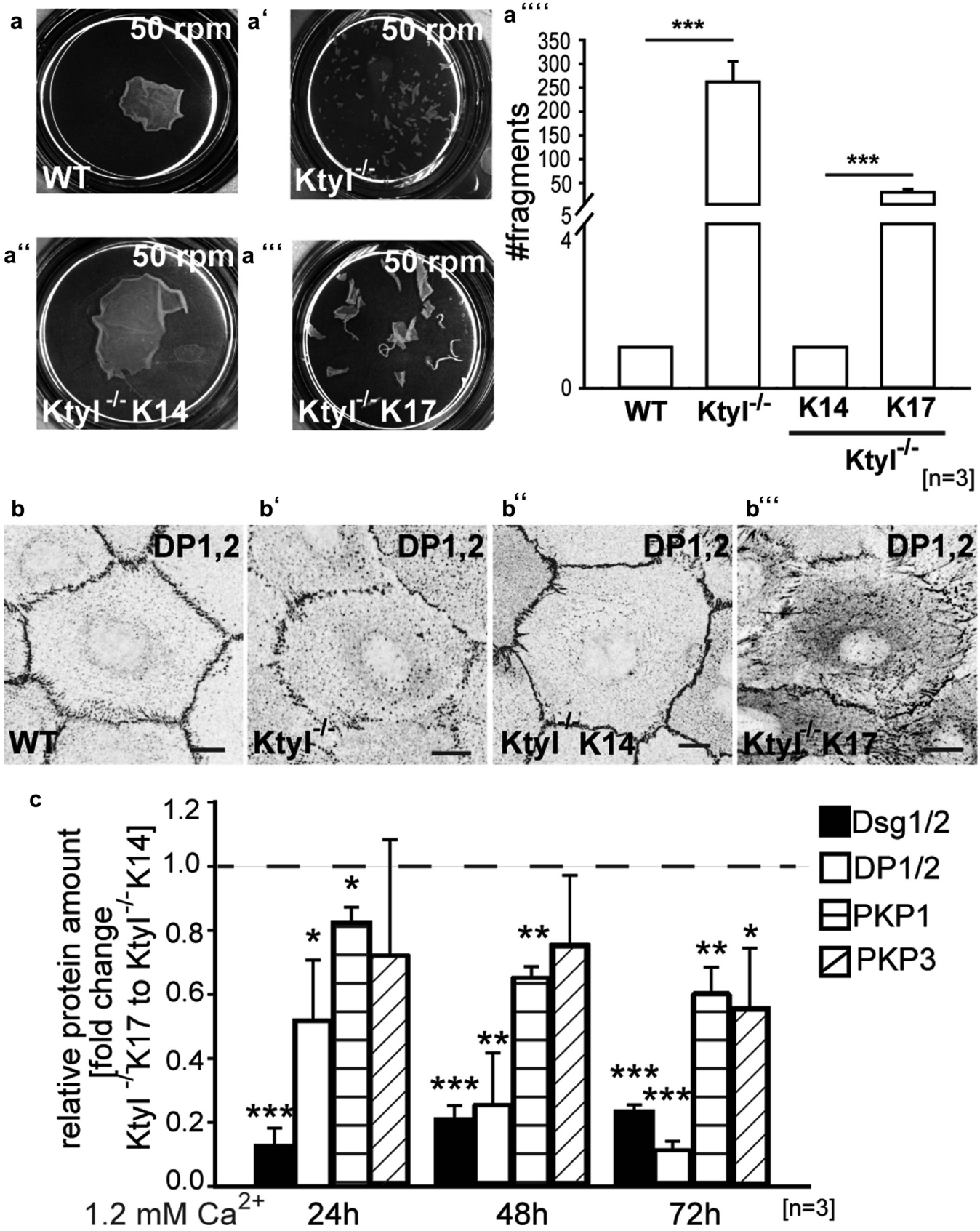

Figure 2. Stability of desmosomes and localization and amount of desmosomal proteins dependent on the keratin-isotype. (**a**–**a**‘‘‘‘) Dispase assay revealed shear stress resilience of WT and K14 cells, whereas Ktyl$^{-/-}$ cells and K17 cells displayed fragmented epithelial sheets under the same conditions (mean ± SEM, n = 3). Although DP1/2 is distributed at the PM in WT (**b**) and K14 cells (**b**‘‘), Ktyl$^{-/-}$ (**b**‘) and K17 cells (**b**‘‘‘) display decreased and irregular PM distribution and accumulation of DP1/2 in the cytoplasm. Scale bars = 10 μm. (**c**) Desmosomal proteins were reduced in K17 compared with K14 cells as analyzed by WB after indicated time points in high calcium medium (mean ± SEM, n = 3). PM, plasma membrane; WB, Western blotting; WT, wild-type.

with K14 cells (Figure 2c, Supplementary Figure S2c–d). The unaltered mRNA levels of desmosomal proteins (Supplementary Figure S2b) indicate that desmosomal protein turnover, but not transcriptional or posttranscriptional control, depends on specific keratin isotypes.

Increased internalization of desmosomes in K17 keratinocytes

Lack of all keratins triggers accelerated internalization of desmosomes and increased degradation of desmosomal proteins (Kroger et al., 2013). Reduced amounts of desmosomal proteins in K17 compared with K14 cells suggested keratin isotype-dependent internalization and degradation. To examine this, junction formation was allowed for 24 hours followed by disruption via EGTA-mediated Ca^{2+}-depletion in both cell lines. One hour after EGTA addition, DP1/2 accumulated in the cytoplasm of K14 and K17 cells, but internalization was much slower in K14 compared with K17 cells (Figure 3a–b′, d). As desmosomes are predominantly internalized through dynamin-dependent endocytosis pathways (Brennan et al., 2012; Delva et al., 2008; Resnik et al., 2011), the dynamin-inhibitor dynasore (Macia et al., 2006) should block desmosome internalization. Indeed, dynasore treatment of K17 cells re-established the distribution of DP1/2 even under conditions of Ca^{2+}-depletion (Figure 3c–c′, d). In further support, surface biotinylation demonstrated an 80% reduction of Dsg1/2 at the PM in K17 cells, restored by dynasore treatment (Figure 3e). To investigate whether Dsg1/2 is internalized faster in K17 cells, surface proteins were biotinylated for 30 minutes. Subsequently, cells were either lysed directly to visualize biotinylated surface proteins at time point 0 or immediately subjected to glutathione stripping to reverse biotinylation. Internalized biotinylated proteins are protected from glutathione stripping. Additionally, cells were incubated in a medium with EGTA for 1 hour and subjected to stripping afterward. This showed that the EGTA-induced internalization of Dsg1/2 relative to its amount at the cell surface, before the addition of EGTA, was greater in K17 compared with K14 cells, even when taking into account that Dsg1/2 surface levels were lower in K17 compared with K14 cells (Figure 3e′; Supplementary Figure S3f online). Dynasore treatment reduced internalization in K17 cells (Figure 3e′, Supplementary Figure S3f). WB of total protein lysates after EGTA treatment confirmed increased degradation of Dsg1/2 in K17 cells, compared with K14 cells (Figure 3f, Supplementary Figure S2e–e″). Dsg1/2 degradation in K17 cells was blocked by treatment with dynasore or inhibitors of protein degradation (chloroquine for lysosomes; lactacystin for proteasomes [Figure 3f, Supplementary Figure S2e–e″]). Furthermore, inhibition of desmosome internalization with dynasore restored adhesion in the dispase assay with K17 cells, whereas inhibition of protein degradation failed to stabilize desmosomes to the same extent (Figure 3g–g‴). This implies that increasing the amount of desmosomal proteins, without stabilization at the plaque, is insufficient to form stable desmosomes in K17 cells. Thus, keratin isotypes primarily are involved in the regulation of the localization, possibly through modulating PTMs of desmosomal proteins (Albrecht et al., 2015), whereas their degradation occurs independently of keratins.

PKCα-mediated induction of desmosome internalization in K17 keratinocytes

PKCα regulates desmosome remodeling after wounding (Thomason et al., 2012; Wallis et al., 2000), and phosphorylation of desmosomal proteins is involved in desmosome assembly and remodeling (Albrecht et al., 2015; Aoyama et al., 2009; Godsel et al., 2005; Hobbs and Green, 2012; Stappenbeck et al., 1994). Previously, we reported that keratins might sequester PKCα through the scaffold protein Rack1, to enable stable desmosome formation (Kroger et al., 2013). Similar to KtyII$^{-/-}$ cells (Kroger et al., 2013), PKCα was enriched in a Dsg1/2-enriched fraction (Figure 4a), which likely represents the membrane fraction (Supplementary Figure S2h), in KtyI$^{-/-}$ and K17 compared with WT and K14 cell extracts (Figure 4a). To test whether K17 is involved in PKCα-mediated destabilization of desmosomes, K17 cells were treated with the PKC-inhibitor Gö6976 (Wallis et al., 2000) and K14 cells with the PKC activator phorbol 12-myristate 13-acetate (PMA). Inhibition of PKCα in K17 cells restored desmosome stability on application of shear stress to an epithelial sheet, whereas PKC activation in K14 cells significantly destabilized epithelial sheets (Figure 4b and Supplementary Figure S2i–i‴). Given its role in regulation of desmosome stability (Hobbs and Green, 2012), the impact of activated PKCα was studied after induction of desmosome internalization by Ca^{2+}-depletion. WB of total protein lysates before and after Ca^{2+}-depletion confirmed increased degradation of Dsg1/2 in PMA-treated K14 cells and partially blocked degradation of Dsg1/2 in K17 cells, treated with Gö6976 (Figure 4c and Supplementary Figure S2g). Activation of PKCα with PMA in K14 cells led to increased internalization of desmosomes, compared with vehicle-treated control cells (Figure 4d and e–f′). In contrast, the treatment of K17 cells with Gö6976 resulted in stabilization of DP1/2 at the PM and slowed down EGTA-induced internalization (Figure 4d and g–h′). In line with the different intracellular and keratin isotype–dependent distribution of PKCα, this suggests that K5/K14 filaments sequester PKCα in the cytoplasm, thereby limiting desmosome internalization, whereas K6/K17 filaments do not prevent accumulation of PKCα to the PM and destabilization of desmosomes. Our data indicate that spatiotemporal PKCα activation after wounding could be mediated by upregulation of K6/K17 in keratinocytes. The well-known regulation of keratin network organization by PTMs (Loschke et al., 2015; Snider and Omary, 2014) raises the question whether keratin isotypes K6/K17 modify desmosome dynamics through regulation of PTMs of desmosomal proteins or by hyperphosphorylation of keratins that might weaken direct interactions with desmosomal proteins. Furthermore, different affinities of K5/K14 and K6/K17 to desmoplakin might modulate desmosome stability. During wound healing, disassembly of cell-cell and cell-matrix contacts initiates keratinocyte migration from the wound edge across the denuded area, whereas keratinocytes behind the migrating front start to proliferate (Pastar et al., 2014; Werner and Grose, 2003). Induction of K6, K16, and K17 expression during re-epithelialization correlates with alterations in cell morphology and migratory properties of keratinocytes (Paladini et al., 1996; Patel et al., 2006). In

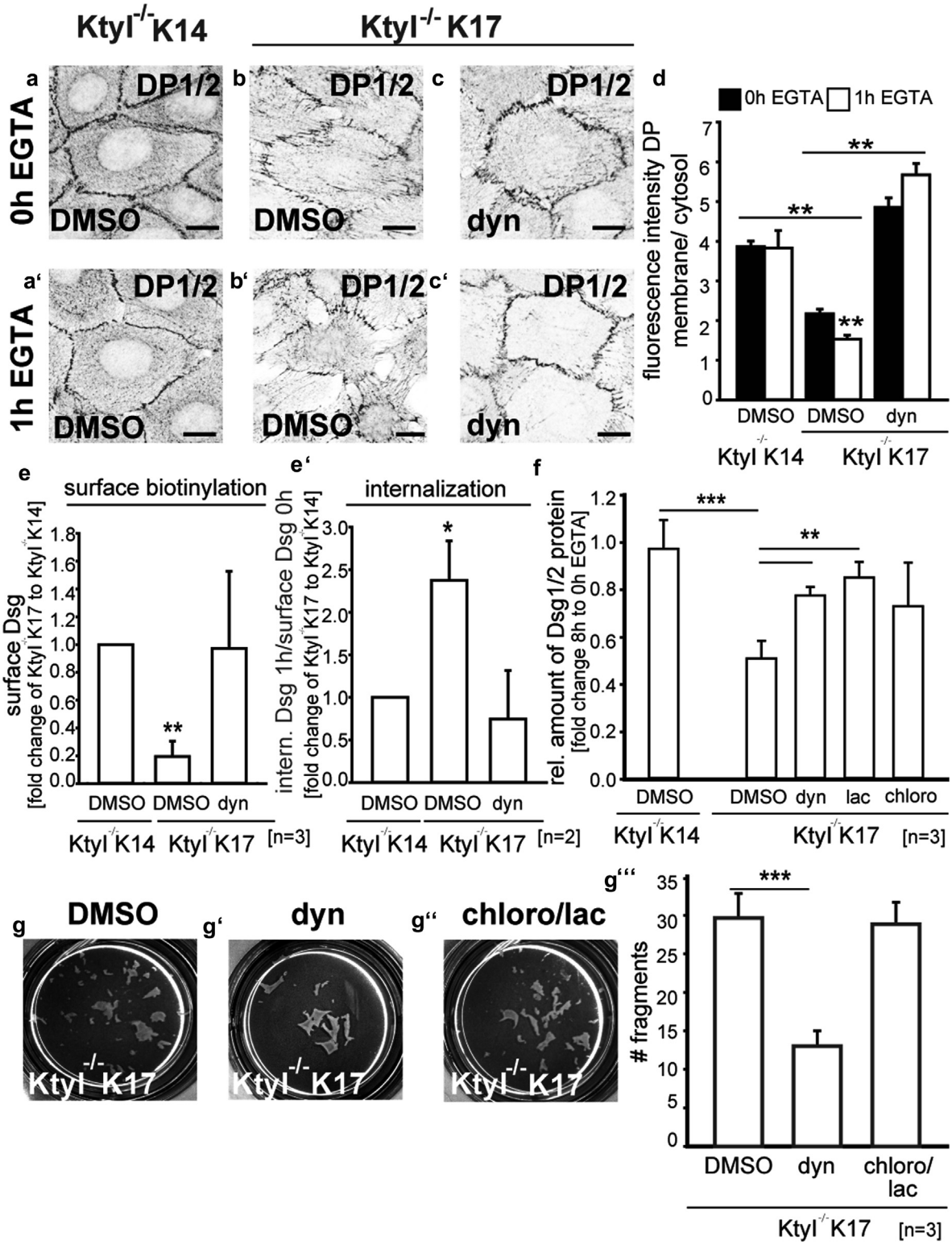

Figure 3. Disassembly and degradation of desmosomes dependent on the keratin-isotype. (**a**–**c**′) Immunostainings for DP1/2 showed accelerated disassembly of desmosomes in K17 compared with K14 cells, both induced by incubation with 2 mM EGTA for 1 hour. Dynasore (dyn) treatment blocks desmosome internalization in K17 cells. Scale bars = 10 μm. (**d**) Ratios of average pixel intensities for DP at PM and cytoplasm (mean ± SEM, n = 50). (**e**) Surface biotinylation and WB showed decreased surface localization of Dsg1/2 in K17 cells, compared with K14 cells, which was restored after dynasore treatment. For the calculation of the relative amount of surface Dsg1/2 tubulin was used as loading control (mean ± SEM, n = 3). (**e**′) Endocytosis assay revealed faster internalization of Dsg1/2 in untreated K17 cells, compared with K14 and K17 cells treated with dynasore. The relative amounts of internalized proteins were quantified as a percentage of the total, initial surface-biotinylated protein pool (mean ± SEM, n = 3). (**f**) Increased degradation of Dsg1/2 in K17 compared with K14 cells after EGTA treatment for 8 hours. Treatment with dynasore (dyn), lactacystin (lac), or chloroquine (chloro) restored Dsg1/2 levels in K17 cells (mean ± SEM, n = 3). (**g**–**g**‴) Increased epithelial sheet stability in the dispase assay after the treatment of K17 cells with dynasore, but not by combined treatment with chloroquine and lactacystin (mean ± SEM, n = 3). DP, desmoplakin; Dsg, desmoglein; PM, plasma membrane; WB, Western blotting.

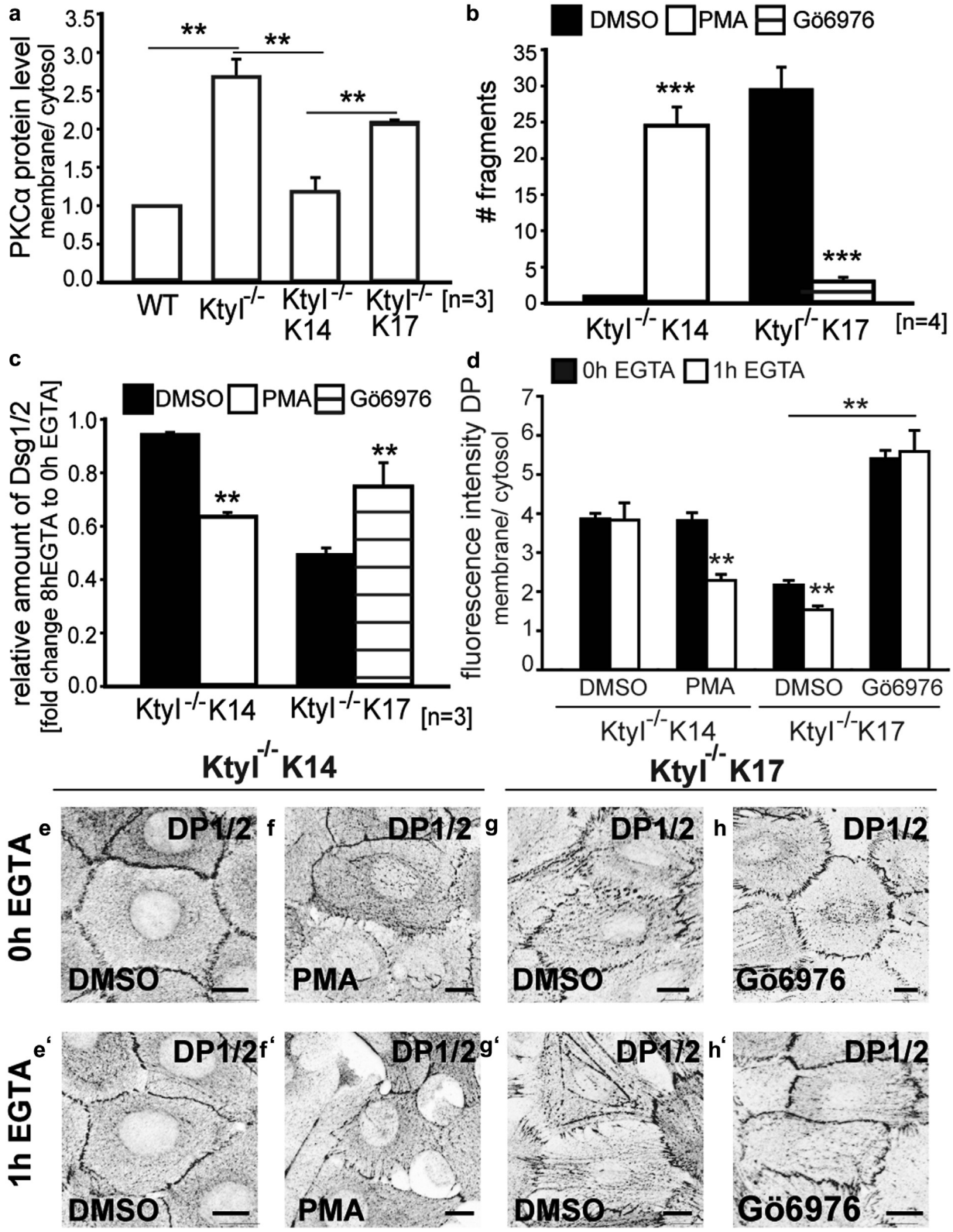

Figure 4. PKCα-activation mediates instability of desmosomes. (**a**) Cell fractionation and WB showed increased PKCα in the PM fraction of Ktyl$^{-/-}$ and K17 cells compared with WT and K14 cells (mean ± SEM, n = 3). (**b**) Activation of PKCα with PMA in K14 cells destabilized desmosomes, whereas blocking PKCα in K17 cells with Gö6976 stabilized epithelial sheets in the dispase assay (mean ± SEM, n = 4). (**c**) WB showed increased degradation of Dsg1/2 in PMA-treated K14 cells after EGTA addition for 8 hours. Inhibition of PKCα in K17 cells slowed down Dsg1/2 degradation. (**d**) Ratios of average pixel intensities for DP at PM and cytoplasm (mean ± SEM, n = 50). (**e**–**h′**) DP1/2 staining on DMSO, PMA, or Gö6976 treatment before and after Ca^{2+} depletion. Desmosome disassembly was accelerated in PMA-treated K14 cells. On Gö6976 treatment of K17 cells, DP1/2 relocalized to the PM and desmosome internalization was decreased. DP, desmoplakin; Dsg, desmoglein; PKCα, protein kinase C alpha; PM, plasma membrane; PMA, phorbol 12-myristate 13-acetate; WB, Western blotting; WT, wild-type. Scale bars = 10 μm.

accordance with this, scratch-wound assays of confluent keratinocyte monolayers revealed a faster collective migration of K17 compared with K14 cells, which correlated with more dynamic desmosomes in those cells. Further, inhibition of PKCα, which stabilizes desmosomes in K17 cells, significantly reduced migration of K17 cells (Supplementary Figure S4a–d online).

K5 protein abundance is crucial to stabilize desmosomes in keratinocytes

To examine whether enhanced internalization and degradation of desmosomal proteins, leading to diminished cell adhesion, depend on the ratio of type II keratins K5:K6 or on the presence of type I keratins K14 and K17, knockdown of K5 or K6 was performed in K14 and K17 cells. Depletion of K5 in K14 cells or K17 cells led to a strong reduction of K5 mRNA and protein, whereas K6, K14, and K17 mRNA and protein levels were unaltered (Figure 5a and Supplementary Figure S3a). In contrast, knockdown of K6 strongly increased K5 protein levels in both cell lines, whereas the amount of K17 protein was significantly reduced in K17 cells (Figure 5b). Quantitative PCR showed that K5 mRNA was slightly reduced (Supplementary Figure S3a′) on K6 knockdown, indicating that in the absence of K6, K5 protein is stabilized. Interestingly, depletion of K5 in K14 cells was accompanied by decreased DP1/2 localization at the PM and its accumulation in the cytoplasm (Figure 4c, c′). Depletion of K5 or K6 did not affect filament organization of residual keratins (Supplementary Figure S3c–e‴). Furthermore, knockdown of K6 in K17 cells partially restored membrane localization of DP1/2 compared with control cells, probably due to the presence of K5/K17 filaments (Figure 4c″, c‴). Knockdown of K5 in K14 cells reduced amounts of Dsg1/2, in agreement with diminished epithelial sheet stability in the dispase assay (Figure 5d–e). Depletion of K6 in K17 cells induced a 2.5-fold increase of Dsg1/2 at the protein level, accompanied by enhanced epithelial sheet stability (Figure 5d–e). These data suggest that the level of K5 relative to K6 in keratinocytes is critical for the formation of stable desmosomes. In further support, transient transfection of a K14 cDNA in K17 cells led to a strong increase of K5 proteins, whereas K6 expression was less affected (Figure 6a–a′). Quantitative PCR showed that mRNA levels of K5, K6, and K17 are not altered after transient transfection of K14 (Supplementary Figure S3b). Expression of K14 and concomitant upregulation of K5 supported increased epithelial sheet integrity during the shear stress assay and increased levels of Dsg1/2 and plakophilin 1, in comparison with mock-transfected K17 cells (Figure 6b–c). Given that the relative abundance of K5 determines desmosome stability, we additionally generated K5 and K6 rescue cell lines, using KtyII$^{-/-}$ cells. Expression of K5 in KtyII$^{-/-}$ cells led to upregulation of K14 and to a lesser extent of K17 (Supplementary Figure S3f). In contrast, expression of K6 in KtyII$^{-/-}$ correlated with higher levels of K17 than K14 protein (Supplementary Figure S3f). Similar to the above data collected in K14 and K17 cells, K5-expressing cells formed stable desmosomes, whereas expression of K6 compromised desmosomal adhesion (Supplementary Figure S3g–h″).

Collectively, our data demonstrate that K5/K14 support stable and highly adhesive desmosomes, whereas K6/K17 render desmosomes more dynamic. Among these keratins, K5 is a major contributor of stable desmosomes (Figure 6d). Our data strongly suggest that keratin isotype composition is the major regulator of desmosome adhesion, yet we cannot rule out that the overall keratin amount expressed also can contribute. Preliminary data suggest that the PKCα-scaffold protein Rack1 (Kroger et al., 2013) interacts with different affinities with K5/K14 and K6/K17 filaments. Others have reported that K6-dependent Src activity modulates keratinocyte migration during tissue repair (Rotty and Coulombe, 2012) and that K17 stimulates cell growth through mTOR in the same setting (Kim et al., 2006). Our observation that expression of K6/K17 decreases intercellular adhesion and renders desmosomes more dynamic strengthens the concept that unique primary sequences of keratin isotypes serve as spatiotemporal signaling scaffolds (Loschke et al., 2015). To which extent stability and function of the keratin-desmosome complex depends on direct protein-protein interactions or on PTMs of both protein family members is now addressable in our keratinocyte culture model. Obviously, the setting during wound healing in vivo is more complex, given that basal and suprabasal cells, which express different keratin pairs, are involved in wound re-epithelialization (Patel et al., 2006). On wounding, the majority of suprabasal cells at the wound edge express K1, K10, K6, K16, and K17, and suprabasal cells migrating onto the wound bed express mainly K6, K16, and K17. In addition, a subpopulation at the wound bed expresses K5, K14, K6, and K17 (Patel et al., 2006). Thus, the availability of K14 and K17 cells provides a unique opportunity to analyze isotype-specific functions of keratins in regulation of junction stability and migration.

MATERIALS AND METHODS

Cell culture

Keratinocytes were cultured as previously described in Kroger et al. (2013) and Ramms et al. (2013). To generate KtyI$^{-/-}$K14, KtyI$^{-/-}$K17, KtyII$^{-/-}$K5, and KtyII$^{-/-}$K6 cells, mouse K14, K17-HA, K5, or K6b cDNAs were cloned into a lentiviral pLVX-Puro vector (Clontech, Saint-Germain en-Laye, France). Respective keratin-free keratinocytes stably expressing constructs were generated by lentiviral transduction essentially as described earlier (Seltmann et al., 2013; Stohr et al., 2012). For experiments, cells were switched to 1.2 mM Ca^{2+}-containing media for 24 hours to 72 hours. A K14-HA construct was subcloned in a pcDNA3.1/Zeo vector (Invitrogen) and transiently transfected in KtyI$^{-/-}$K17 cells. For knockdown experiments siK5, siK6 (targeting K6a and b) and control siRNA were purchased as SMARTpool containing four individual siRNAs from Dharmacon (Thermo Scientific). Plasmids and siRNAs were transfected using Xfect (Clontech, Saint-Germain en-Laye, France) following the manufacturer's protocol.

EGTA and drug treatment

EGTA treatment was performed as described previously in Kroger et al. (2013). Drugs are listed in Supplementary Table S1 online.

Immunofluorescence

Fixation of cells and staining was performed as previously described in Kroger et al. (2013). Antibodies are listed in Supplementary Table S2 online.

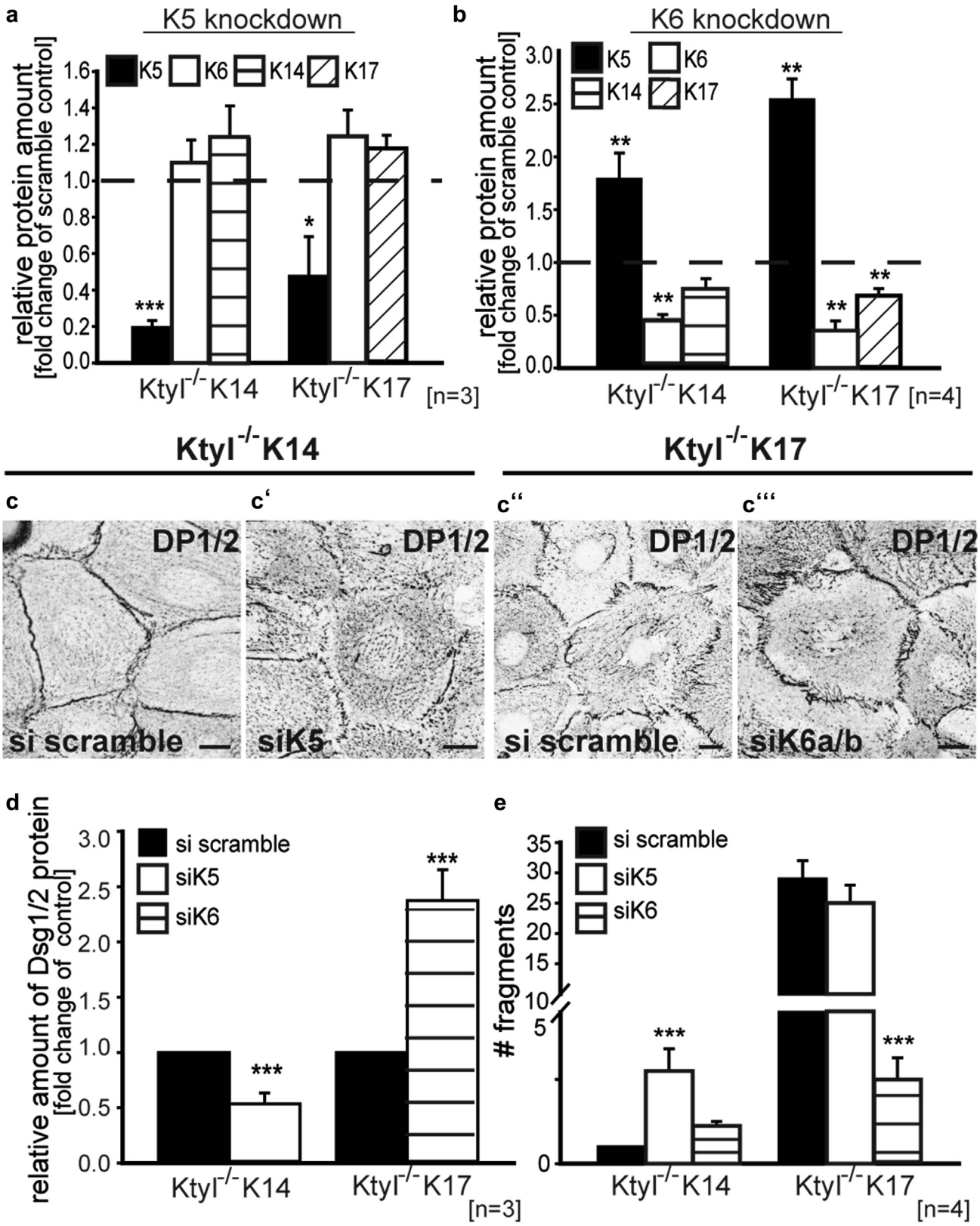

Figure 5. Ratio of K5/K14 versus K6/K17 protein levels determines desmosome stability. (**a**) WB showed a strong reduction of the K5 protein level 48 hours after K5 knockdown. Note unaltered K6, K14, and K17 levels (mean ± SEM, n = 3). (**b**) K6 knockdown caused upregulation of K5 in K14 and K17 cells and downregulation of K17 in K17 cells, whereas the K14 level in K14 cells remained unaffected. (**c**–**c**‴) Reduction of DP1/2 at the PM K14 cells on K5 knockdown and relocalization of DP1/2 to the PM in K17 cells after K6 knockdown. Scale bars = 10 μm. (**d**) Decreased Dsg1/2 protein level after K5 knockdown in K14 cells and increased Dsg1/2 level in K17 cells on K6 knockdown (mean ± SEM, n = 3). (**e**) K5 knockdown decreased sheet stability in K14 cells and K6 knockdown increased sheet stability in K17 cells (dispase assay; mean ± SEM, n = 4). DP, desmoplakin; Dsg, desmoglein; PM, plasma membrane; WB, Western blotting.

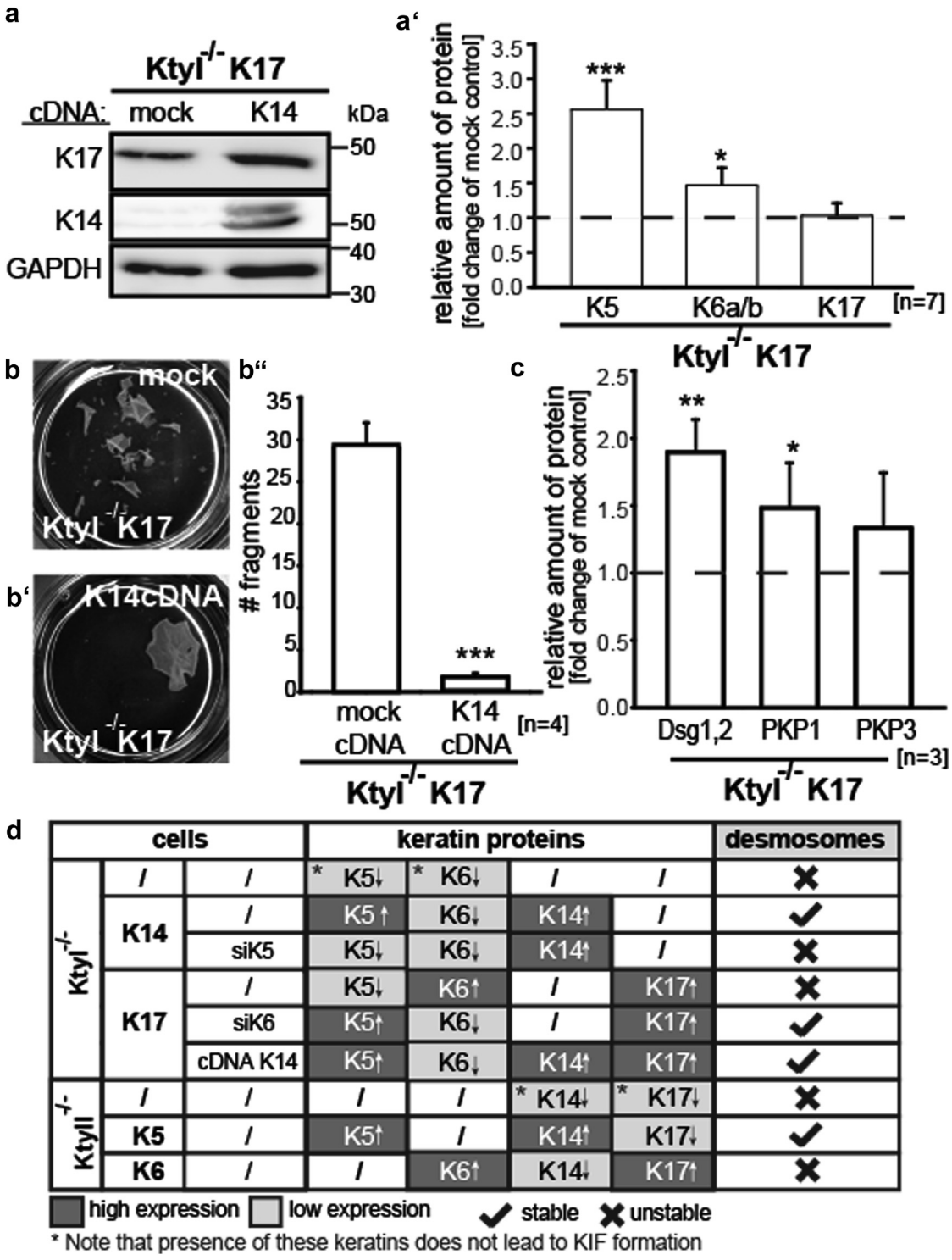

Figure 6. Keratin-isotype dependent stability of desmosomes. (**a**–**a**′) WB validated expression of K14 in K17 cells, after transient transfection with K14 cDNA. Compared with mock-transfected controls, transient transfection with K14 increased K5 and K6 levels without affecting K17 protein levels (mean ± SEM, n = 7). (**b**–**b**″) Transient transfection of K14 into K17 cells increased the stability of epithelial sheets in the dispase assay (mean ± SEM, n = 4). (**c**) Re-expression of K14 in K17 cells increased amounts of Dsg1/2, PKP1, and PKP3 (mean ± SEM, n = 3). (**d**) Table showing that desmosome stability coincides with the presence of high protein levels of K5. Dsg, desmoglein; PKP, plakophilin; WB, Western blotting.

Immunofluorescence microscopy and data processing

Image stacks were collected with a Zeiss LSM 780 confocal microscope equipped with 40/1.3 NA or 63/1.46 NA oil immersion objectives. Image analysis and processing were performed using Zen Software 2010 (Carl Zeiss, Jena, Germany), Zen Blue Software (Carl Zeiss, Jena, Germany), and Photoshop CS4 (Adobe) software. Lookup table (brightness) was adjusted using Photoshop.

Western blotting

SDS-PAGE and WB was performed as described (Vijayaraj et al., 2009). Antibodies are listed in Supplementary Table S2.

RNA preparation and real-time PCR

Confluent cell monolayers were homogenized in TRIzol (Invitrogen) supplemented with ribonucleoside-vanadyl complexes at 5 mM final concentration (NewEngland BioLabs). Total RNA was phenol and/or chloroform extracted and precipitated followed by DNaseI treatment (Fermentas Life Science). cDNA synthesis was carried out using a RevertAid H Minus First Strand cDNASynthesis kit (Fermentas Life Science). Real-time PCR was performed with a Maxima SYBRGreen/ROX qPCR Master Mix (Fermentas Life Science) and run on an Applied Biosystems 7500 Real Time PCR system. All samples were normalized against glyceraldehyde-3-phosphate dehydrogenase mRNA, and results are reported as *n*-fold change relative to the respective control. Primer pairs are listed in Supplementary Table S3 online. PCR conditions were as follows: 95 °C for 15 minutes, followed by 40 cycles of 95 °C for 15 seconds, 60 °C for 30 seconds, and 72 °C for 35 seconds.

Surface biotinylation

A total of 3×10^5 cells per well were seeded on a six-well plate. Twenty-four hours after plating, the medium was switched to a high calcium medium for 24 hours. Cells were washed three times with ice-cold PBS Mg/Ca and surface-labeled for 30 minutes with cell-impermeable EZ-Link Sulfo-NHS-SS-Biotin (Pierce) (1.5 mg/ml) following the manufacturer's instructions on ice. Cells were washed three times with PBS Mg/Ca containing 100 mM glycine for 20 minutes on ice to quench residual biotin. For cell surface measurements, cells were lysed with 500 µl of cold RIPA buffer pH 7.5, with 1× protease and phosphatase inhibitor cocktails (Pierce). Lysates were incubated with 50 µl streptavidin beads (Pierce) for 1 hour. Beads were washed four times with 800 µl of cold RIPA buffer pH 7.5, with 1× protease and phosphatase inhibitor cocktails. Biotinylated PM proteins were finally eluted by SDS-PAGE buffer and subsequently analyzed by WB. The amount of membrane-bound Dsg2 was calculated as the ratio of biotinylated protein to tubulin in the input fraction. To measure internalization, cells were labeled with biotin as described before and incubated for 1 hour with a low-calcium medium containing 3 mM EGTA. Subsequently, surface biotin was stripped by three 20-minute washes of stripping solution (100 mM MESNA, 50 mM Tris-HCl, pH 8.6, 100 mM NaCl, 1 mM EDTA, and 0.2% BSA) at 4 °C, and one 10-minute wash with 120 mM iodoacetamide in PBS Mg/Ca. After stripping, cells were lysed in 500 µl of cold RIPA buffer and incubated with beads. The effectiveness of glutathione stripping was demonstrated by surface-biotinylation at 4 °C for 30 minutes, followed by immediate glutathione stripping. Only internalized biotinylated proteins protected from glutathione stripping could be precipitated with neutravidin beads and analyzed by immunoblotting.

Cell fractionation

The assay was performed as described in Kroger et al. (2013).

Dispase assay

The assay was performed as described in Calautti et al. (1998) and Kroger et al. (2013).

Statistical analysis

Statistical significance was determined by two-tailed *t*-tests. When equal variance test failed, the Wilcoxon-Mann-Whitney rank sum test was run (*$P = 0.05$; **$P = 0.01$; ***$P = 0.005$).

CONFLICT OF INTEREST

The authors state no conflict of interest.

ACKNOWLEDGMENTS

We thank Stefan Hüttelmaier and Marcell Lederer (Universitätsklinikum Halle, Halle, Germany) for production of lentivirus and transduction of cells. Work in the Magin lab is supported by the Deutsche Forschungsgemeinschaft (MA-1316/9-3, 1316/15-1, 1316/17-1; MA1316/19-1, MA1316/21-1, MA1316/22-1) and the Translational Center for Regenerative Medicine, TRM, Leipzig, PtJ-Bio, 0315883, to TMM.

SUPPLEMENTARY MATERIAL

Supplementary material is linked to the online version of the paper at www.jidonline.org, and at doi:10.1038/JID.2015.403.

REFERENCES

Albrecht LV, Zhang L, Shabanowitz J, et al. GSK3- and PRMT-1-dependent modifications of desmoplakin control desmoplakin-cytoskeleton dynamics. J Cell Biol 2015;208:597–612.

Aoyama Y, Yamamoto Y, Yamaguchi F, et al. Low to high Ca^{2+}-switch causes phosphorylation and association of desmocollin 3 with plakoglobin and desmoglein 3 in cultured keratinocytes. Exp Dermatol 2009;18:404–8.

Bar J, Kumar V, Roth W, et al. Skin fragility and impaired desmosomal adhesion in mice lacking all keratins. J Invest Dermatol 2014;134:1012–22.

Brennan D, Peltonen S, Dowling A, et al. A role for caveolin-1 in desmoglein binding and desmosome dynamics. Oncogene 2012;31:1636–48.

Calautti E, Cabodi S, Stein PL, et al. Tyrosine phosphorylation and src family kinases control keratinocyte cell-cell adhesion. J Cell Biol 1998;141:1449–65.

Delva E, Jennings JM, Calkins CC, et al. Pemphigus vulgaris IgG-induced desmoglein-3 endocytosis and desmosomal disassembly are mediated by a clathrin- and dynamin-independent mechanism. J Biol Chem 2008;283:18303–13.

Garrod DR, Berika MY, Bardsley WF, et al. Hyper-adhesion in desmosomes: its regulation in wound healing and possible relationship to cadherin crystal structure. J Cell Sci 2005;118:5743–54.

Godsel LM, Hsieh SN, Amargo EV, et al. Desmoplakin assembly dynamics in four dimensions: multiple phases differentially regulated by intermediate filaments and actin. J Cell Biol 2005;171:1045–59.

Gurtner GC, Werner S, Barrandon Y, et al. Wound repair and regeneration. Nature 2008;453:314–21.

Hatzfeld M, Franke WW. Pair formation and promiscuity of cytokeratins: formation in vitro of heterotypic complexes and intermediate-sized filaments by homologous and heterologous recombinations of purified polypeptides. J Cell Biol 1985;101:1826–41.

Hesse M, Zimek A, Weber K, et al. Comprehensive analysis of keratin gene clusters in humans and rodents. Eur J Cell Biol 2004;83:19–26.

Hobbs RP, Green KJ. Desmoplakin regulates desmosome hyperadhesion. J Invest Dermatol 2012;132:482–5.

Homberg M, Magin TM. Beyond expectations: novel insights into epidermal keratin function and regulation. Int Rev Cell Mol Biol 2014;311:265–306.

Homberg M, Ramms L, Schwarz N, et al. Distinct impact of two keratin mutations causing epidermolysis bullosa simplex on keratinocyte adhesion and stiffness. J Invest Dermatol 2015;135:2437–45.

Kim S, Wong P, Coulombe PA. A keratin cytoskeletal protein regulates protein synthesis and epithelial cell growth. Nature 2006;441:362–5.

Kroger C, Loschke F, Schwarz N, et al. Keratins control intercellular adhesion involving PKC-alpha-mediated desmoplakin phosphorylation. J Cell Biol 2013;201:681–92.

Loschke F, Seltmann K, Bouameur JE, et al. Regulation of keratin network organization. Curr Opin Cell Biol 2015;32C:56–64.

Macia E, Ehrlich M, Massol R, et al. Dynasore, a cell-permeable inhibitor of dynamin. Dev Cell 2006;10:839–50.

Magin TM, Vijayaraj P, Leube RE. Structural and regulatory functions of keratins. Exp Cell Res 2007;313:2021–32.

McHarg S, Hopkins G, Lim L, et al. Down-regulation of desmosomes in cultured cells: the roles of PKC, microtubules and lysosomal/proteasomal degradation. PloS One 2014;9:e108570.

Paladini RD, Takahashi K, Bravo NS, et al. Onset of re-epithelialization after skin injury correlates with a reorganization of keratin filaments in wound edge keratinocytes: defining a potential role for keratin 16. J Cell Biol 1996;132:381–97.

Pan X, Hobbs RP, Coulombe PA. The expanding significance of keratin intermediate filaments in normal and diseased epithelia. Curr Opin Cell Biol 2013;25:47–56.

Pastar I, Stojadinovic O, Yin NC, et al. Epithelialization in wound healing: a comprehensive review. Adv Wound Care (New Rochelle) 2014;3:445–64.

Patel GK, Wilson CH, Harding KG, et al. Numerous keratinocyte subtypes involved in wound re-epithelialization. J Invest Dermatol 2006;126:497–502.

Ramms L, Fabris G, Windoffer R, et al. Keratins as the main component for the mechanical integrity of keratinocytes. Proc Natl Acad Sci USA 2013;110:18513–8.

Resnik N, Sepcic K, Plemenitas A, et al. Desmosome assembly and cell-cell adhesion are membrane raft-dependent processes. J Biol Chem 2011;286:1499–507.

Rotty JD, Coulombe PA. A wound-induced keratin inhibits src activity during keratinocyte migration and tissue repair. J Cell Biol 2012;197:381–9.

Seltmann K, Roth W, Kroger C, et al. Keratins mediate localization of hemidesmosomes and repress cell motility. J Invest Dermatol 2013;133:181–90.

Shaw TJ, Martin P. Wound repair at a glance. J Cell Sci 2009;122:3209–13.

Simpson CL, Patel DM, Green KJ. Deconstructing the skin: cytoarchitectural determinants of epidermal morphogenesis. Nat Rev Mol Cell Biol 2011;12:565–80.

Snider NT, Omary MB. Post-translational modifications of intermediate filament proteins: mechanisms and functions. Nat Rev Mol Cell Biol 2014;15:163–77.

Stappenbeck TS, Lamb JA, Corcoran CM, et al. Phosphorylation of the desmoplakin COOH terminus negatively regulates its interaction with keratin intermediate filament networks. J Biol Chem 1994;269:29351–4.

Stohr N, Kohn M, Lederer M, et al. IGF2BP1 promotes cell migration by regulating MK5 and PTEN signaling. Genes Dev 2012;26:176–89.

Thomason HA, Cooper NH, Ansell DM, et al. Direct evidence that PKC-alpha positively regulates wound re-epithelialization: correlation with changes in desmosomal adhesiveness. J Pathol 2012;227:346–56.

Vijayaraj P, Kroger C, Reuter U, et al. Keratins regulate protein biosynthesis through localization of GLUT1 and -3 upstream of AMP kinase and Raptor. J Cell Biol 2009;187:175–84.

Wallis S, Lloyd S, Wise I, et al. The alpha isoform of protein kinase C is involved in signaling the response of desmosomes to wounding in cultured epithelial cells. Mol Biol Cell 2000;11:1077–92.

Werner S, Grose R. Regulation of wound healing by growth factors and cytokines. Physiol Rev 2003;83:835–70.

Windoffer R, Beil M, Magin TM, et al. Cytoskeleton in motion: the dynamics of keratin intermediate filaments in epithelia. J Cell Biol 2011;194:669–78.